Food Chemistry: X 24 (2024) 101943

Contents lists available at ScienceDirect

Food Chemistry: X

journal homepage: www.sciencedirect.com/journal/food-chemistry-x

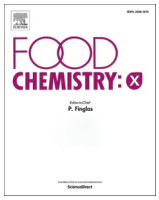

Feasibility analysis on the application of the Maillard reaction in developing *Lentinula edodes* umami seasoning: Based on the umami substances, sensory quality, physicochemical properties of the products

Jianguo Qiu [a], Hongyu Li [a], Lijia Zhang [a], Junqi Li [a], Zhengfeng Fang [a], Cheng Li [a], Hong Chen [a], Fahad Al-Asmari [b], Manal Y. Sameeh [c], Wenjuan Wu [d], Yuntao Liu [a,*], Zhen Zeng [a,*]

[a] College of Food Science, Sichuan Agricultural University, Ya'an 625014, China
[b] Department of Food and Nutrition Sciences, College of Agricultural and Food Sciences, King Faisal University, Al Ahsa, 31982, Saudi Arabia
[c] Department of chemistry, Al-Leith University College, Umm Al Qura University, Makkah 25100, Saudi Arabia
[d] College of Science, Sichuan Agricultural University, Yaan 625014, China

ARTICLE INFO

Keywords:
Umami substances
Maillard reaction
Sensory quality
Physicochemical properties

ABSTRACT

To elucidate the feasibility of applying the Maillard reaction (MR) to the development of *Lentinula edodes* umami seasoning, this study quantitatively analyzed the main umami substances in the products and evaluated their sensory quality. Simultaneously, the rheology, thermal stability, zeta potential, and particle size of the products were also studied. The results indicated that after the MR, the content of umami amino acids in *Lentinula edodes* hydrolysates (LEHs) decreased from 17.72 mg/g to 12.70 mg/g, while the content of umami nucleotides increased from 0.61 mg/g to 1.36 mg/g. The equivalent umami concentration of MR products was high, at 293.84 ± 11.05 g MSG/100 g. Taste activity value indicated that 5'-GMP, Asp, and Glu were the key umami substances. MR increased the umami sensory score, particle size, absolute zeta potential, and viscosity of LEHs, and altered their thermal stability. These results support the application of MR in the mushroom umami seasoning.

1. Introduction

Lentinula edodes are an excellent food resource rich in nutrients and possessing various biological activities (Chen, Gao, et al., 2021; Qiu et al., 2024). Particularly, *Lentinula edodes* possess a delicious flavor and contain various umami compounds, such as Aspartic acid, glutamic acid, 5′-guanosine monophosphate, 5′-inosine monophosphate, 5′-adenosine monophosphate, and succinic acid (Chen, Jiang, et al., 2021; Sun et al., 2020). Umami taste is a basic taste of human beings (Andres-Hernando et al., 2021). Umami can increase consumers' appetite and enhance the acceptance of food (Zhao et al., 2019). Therefore, *Lentinula edodes* are commonly employed for the development of natural umami seasonings.

The enzymatic hydrolysate of edible fungi is used as a substrate, with the addition of extra sugars or amino acids, and subjected to the MR under appropriate high temperatures. This approach is considered an effective method for enhancing the umami quality of flavoring bases derived from edible fungi (Sun et al., 2020; Zhang et al., 2019). Zhang et al. (Zhang et al., 2022) discovered that the MRPs obtained from the reaction of *Pleurotus citrinopileatus hydrolysates* with xylose and cysteine received the highest umami sensory scores, exhibiting a rich meaty flavor and kokumi taste. Chen et al. observed that the MRPs derived from *Craterellus tubaeformis* hydrolysates, when subjected to a reaction temperature of 125 °C, achieved the highest sensory scores in terms of both continuity and umami flavor (Chen et al., 2018). In our previous study (Qiu et al., 2024), we utilized non-targeted metabolomics in conjunction with human sensory evaluation to elucidate the impact of the MR on the flavor profile of *Lentinula edodes hydrolysates* (LEHs). The study revealed that after the MR, the relative concentrations of differential metabolites such as amino acids, nucleotides, and succinic acid in LEHs underwent varying degrees of change. The MRPs have a high level of umami intensity and overall acceptability. However, the aforementioned studies did not quantify the umami compounds in the products

Abbreviations: MR, Maillard reaction; MRPs, Maillard reaction products; HPLC, high-performance liquid chromatography; DSC, differential scanning calorimetry; PCA, principal component analysis; LDA, linear discriminant analysis; PDI, polydispersity index.

* Corresponding author at: College of Food Science, Sichuan Agricultural University, 46# Xinkang Road, Yaan, Sichuan 625014, China.
E-mail addresses: liuyt@sicau.edu.cn (Y. Liu), 14399@sicau.edu.cn (Z. Zeng).

https://doi.org/10.1016/j.fochx.2024.101943
Received 4 September 2024; Received in revised form 28 October 2024; Accepted 28 October 2024
Available online 1 November 2024

before and after the MR, nor did they identify the key umami substances.

HPLC and enzyme-linked immunosorbent assay kits are commonly used for the quantitative analysis of substances. The equivalent umami concentration (EUC) can be employed to evaluate the umami intensity of the products (Wang et al., 2023; Yang et al., 2022). The EUC reflects the synergistic effects of umami amino acids and umami nucleotides. The taste activity value (TAV) is the ratio of the concentration of taste compounds to their taste thresholds, and TAV can reveal the key umami compounds in the products (Wang et al., 2023; Yang et al., 2022). Electronic sensory analysis and human sensory evaluation can provide a comprehensive reflection of the umami intensity and sensory quality of the products (Habinshuti et al., 2021). Therefore, the aforementioned methods can be utilized to analyze the impact of the MR on the umami intensity and overall sensory quality of *Lentinula edodes* umami seasoning (Phat et al., 2016).

The impact of the MR on the physicochemical properties of products is also a focus in the field of food processing. The rheological characteristics, thermal stability, particle size, and zeta potential of the products are related to the stability during the processing of *Lentinula edodes* umami seasoning and the drying and heating methods employed (Altay et al., 2024; Chen, Gao, et al., 2021; Zheng et al., 2023). A comprehensive understanding of these attributes can aid in optimizing subsequent production applications. Chen et al. (Chen, Jiang, et al., 2021) used DSC and dynamic light scattering to analyze the thermal stability and zeta potential of MRPs derived from chicken liver protein hydrolysates. They found that the exhibited multiple endothermic peaks due to their complex composition, and the zeta potential results indicated that the MRPs were negatively charged. Zhang et al. (Zhang et al., 2022). found that the particle size of the products from the MR model of *Pleurotus citrinopileatus* hydrolysates/xylose/cysteine was the smallest (0.89 ± 0.01 μm). In conclusion, these results provide a solid theoretical basis for the production and application of the MR in seasonings.

To elucidate the feasibility of applying the MR to *Lentinula edodes* umami seasoning, the objectives of this study were: (1) to quantitatively analyze the major umami compounds (umami amino acids, umami nucleotides, and succinic acid) in LEHs and their MRPs; (2) to comprehensively evaluate the impact of the MR on the umami intensity and sensory quality of LEHs based on EUC values, TAV, electronic sensory analysis, and human sensory evaluation; (3) to characterize the physicochemical properties (rheology, thermal stability, zeta potential, and particle size) of LEHs and their MRPs, providing a reference for subsequent production of *Lentinula edodes* umami seasoning.

2. Materials and methods

2.1. Materials and chemical reagents

Lentinula edodes specimens, which had a cultivation cycle spanning approximately eight months, exhibited a compact stipe and a round, plump, and fleshy pileus. The margin of the pileus was notably large and curled, with deep fissures and a naturally occurring pattern. The gills were well-ordered, and the cap opened to a degree of ≤7, presenting a greyish-white hue. The diameter of these specimens was approximately between 3 and 5 cm, and their external shape is depicted in Supplementary Material 1: Fig. S1. These specimens were purchased from a market selling edible mushrooms in Lizhou, Sichuan Province, China. Food-grade composite cellulase (20,000 U/g) and food-grade composite protease (50,000 U/g) were obtained from Zhejiang Yinuo Science and Technology Co., Ltd. D-xylose and L-cysteine were supplied by Henan Wanbang Industrial Co., Ltd., and perchloric acid, phosphate buffer, sodium hydroxide, acetonitrile, methanol, and other reagents from Sinopharm Chemical Reagent Co., Ltd. The succinic acid assay kit was supplied by Shanghai Enzyme-linked Biotechnology Co., Ltd. Monosodium glutamate was bought from a local supermarket in Yucheng District, Ya'an City. Standards like 5′-cytidine monophosphate (5'-CMP), 5′-uridine monophosphate (5'-UMP), 5′-inosine monophosphate (5'-IMP), 5′-guanosine monophosphate (5'-GMP), 5′-adenosine monophosphate (5'-AMP), ADP, HxR, Hx, ATP, and amino acid standards were bought from Shanghai Yuan Ye Biological Technology Co., Ltd.

2.2. The preparation of the samples

Preparation methods for these three samples were consistent with those used in our previous research (Qiu et al., 2024). The preparation is as follows:

The dried *Lentinula edodes* were initially processed using a universal grinder to achieve a fine powder. The powdered material was then subjected to sieving through a 40-mesh sieve to ensure uniform particle size. 2 g of the powdered *Lentinula edodes* were combined with 40 g of ultrapure water, maintaining a solid-to-liquid ratio of 1:20 (*w/v*). The mixture was subsequently subjected to magnetic stirring at a temperature of 50 °C for a duration of 1 h. Following this, the solution was centrifuged at 6000 rpm for 10 min to remove particulate matter. The resultant *Lentinula edodes* water extract served as the control (Control) and was subsequently stored at −20 °C in a freezer for subsequent applications.

The pH of the water extract was adjusted to the optimal pH of the cellulase (pH = 4.5) using 2 M HCl/NaOH. Subsequently, cellulase (3 % w/w) was added to the solution, followed by magnetic stirring at 45 °C for 2 h. The enzyme solution was then inactivated by boiling for 15 min. The pH of the mixture was subsequently adjusted to the optimal pH for the composite protease (pH = 6) using 2 M HCl/NaOH. The composite protease (4 % w/w) was then added, and the mixture was stirred magnetically at 50 °C for 2 h. Upon completion of the enzymatic hydrolysis, the hydrolyzed solution was boiled for 15 min to denature the enzymes. The enzymatically hydrolyzed solution was then centrifuged at 6000 rpm for 10 min to obtain the *Lentinus edodes* hydrolysates (LEHs). Finally, the LEHs were stored at −20 °C in a freezer for use in subsequent experiments.

A mixture was prepared by combining 0.4 g of D-xylose, 0.24 g of L-cysteine, and 80 mL of LEHs. Simultaneously, the pH of the mixture was adjusted to 6.5 using 2 M HCl/NaOH. The mixture was then transferred to a reaction vessel equipped with a magnetic stirrer and heated to 120 °C in an oil bath for 100 min under a sealed condition. Upon completion of the process, the mixture was centrifuged at 6000 rpm for 10 min. The products obtained through the MR were designated as MRPs. The MRPs were stored in a freezer at −20 °C for subsequent use.

2.3. Quantification of free amino acids

The experimental method was adapted from the approach of Manninen et al. (Manninena et al., 2018). Quantification of free amino acids was done through HPLC with an Agilent 1100 liquid chromatography system having a VWD detector. Prior to analysis, the sample solutions underwent pre-column derivatization with OPA-FMOC. The chromatographic column used was a Zorbax Eclipse-AAA column (4.6 mm × 150 mm, 3.5 μm), kept at 45 °C. Detection signal was monitored by a UV detector at wavelengths of 338 nm (0–19 min) and 266 nm (19.01–25 min). The mobile phase A consisted of a 40 mmol/L phosphate buffer (pH = 7.8), whereas mobile phase B was a mixture of acetonitrile: methanol: water (45:45:10, v/v/v), filtered by the 0.22 μm membrane before being used. The flow rate was set at 1 mL/min. Quantification was achieved using a calibration curve obtained from amino acid standards (Supplementary Material 2).

2.4. Quantification of free nucleotides

The experimental methodology was referenced from Manninen et al. with modifications (Manninena et al., 2018). Took 2 mL of sample solution, diluted it 5 times with perchloric acid, shook thoroughly, centrifuged at 4000 r/min for 15 min, and collected the supernatant. Utilized pH paper to indicate, adjusted pH of the solution to 6.7 by 5

mol/L sodium hydroxide, then made up the volume with double-distilled water, shook well, let stand at 4 °C for 30 min, and then filtered via the 0.22 μm aqueous system filter syringe into a sample vial for HPLC (Agilent 1100 Liquid Chromatograph, USA) analysis. The chromatographic detection conditions involved the use of a GRACE Smart C18 column from the United States (250 mm × 4.6 mm, 5 μm) with a column temperature of 40 °C, a flow rate of 1.0 mL/min, a detection wavelength of 260 nm, and an injection volume of 10 μL. Quantification was performed using a calibration curve of nucleotide standard samples. The separation process utilized gradient elution, with the specific conditions outlined in the appendix materials (Supplementary Material 3).

2.5. Quantification of succinic acid

Succinic acid was detected using an enzyme-linked immunosorbent assay kit method, where the color shade of the sample was negatively correlated with the succinic acid content of the sample. The operational steps were as follows: (1) The samples were repeatedly frozen and thawed at −20 °C, then filtered through glass fiber and set aside. (2) Added samples: Set up standard wells, blank wells (which serve as blank controls without any samples or enzyme-labeled reagents, though all other steps are identical), and test sample wells. To the standard wells of the enzyme-linked immunosorbent assay (ELISA) plate, add 50 μL of the test sample (first add 40 μL of sample diluent—PBS with 5 % bovine serum albumin, pH = 7.2—to the well, then add 10 μL of the test sample). When adding the sample, place it at the bottom of the ELISA plate well without touching the well walls, and gently shake to ensure even mixing. (3) Added enzyme (HRP-labeled anti-IgG antibody): Except for the blank wells, 50 μL enzyme-labeled reagent was poured into every well. (4) Incubation: Sealed the plate utilizing a sealing film and incubated for 60 min at 37 °C. (5) Preparation of solution: Diluted the concentrated dilution (PBS containing 0.05 % Tween 20, pH = 7.2) 30 times. (6) Washing: Carefully removed the sealing film, threw away the liquid, flicked dry, filled every well with washing solution, let stand for 30 s, later discarded and repeated this process 5 times, and tapped dry. (7) Color development: Added 50 μL color developer A (Contains 30 % hydrogen peroxide) and then 50 μL color developer B (Tetramethylbenzidine) to every well, softly shook to mix, and developed color in the dark at 37 °C for 15 min. (8) Termination: Poured 50 μL stop solution (1 M H_2SO_4) into every well to cease the reaction (the color changed from blue to yellow immediately). (9) Measurement: Zeroed the instrument with the blank well, then measured the absorbance (OD value) of every well at 450 nm as the wavelength (Varioskan LUX, Thermo Fisher Scientific Co., Ltd., Shanghai, China). The measurement was conducted within 15 min after adding the stop solution. Finally, calculated the content of succinic acid using the standard curve ($y = -0.0017\times + 0.7963$, $R^2 = 0.9949$) (Supplementary Material 1).

2.6. Calculation of EUC and TAV

2.6.1. EUC value

The calculation of EUC value is done according to the formula below (Yang et al., 2022):

$$Y = \left(\sum a_i b_i\right) + 1218\left(\sum a_i b_i\right)\left(\sum a_j b_j\right)$$

Y represents the EUC of the sample (expressed as g MSG/100 g); a_i denotes the concentration (g/100 g) of each umami amino acid (Glu or Asp); a_j indicates the concentration (g/100 g) of each umami 5′-nucleotide (5'-GMP, 5'-AMP, or 5'-IMP); b_i is the relative umami concentration of each amino acid (Asp, 0.077 and Glu, 1); b_j is the relative umami concentration of each 5′-nucleotide (5'-AMP, 0.18; 5'-GMP, 2.3; and 5'-IMP, 1); and 1218 is the synergy constant based on the concentrations used (g/100 g).

2.6.2. TAV

The calculation of TAV is done on basis of the formula below (Wang et al., 2023; Yang et al., 2022):

$$TAV = \frac{C_1}{C_2}$$

C_1 represents the concentration of the taste compound, while C_2 denotes the threshold concentration of the taste compound.

2.7. Electronic nose analysis

The electronic nose detection method, modified from the research method of Kong et al. (2024), was employed. The detection was performed using a PEN3 electronic nose (PEN3, AIRSENSE Co., Ltd., Schwerin, Germany). A 2 mL sample (freeze-dried sample was configured to a concentration of 10 mg/mL) was placed into a 20 mL sampling bottle and then heated in a constant temperature environment at 50 °C for 10 min. Subsequently, the probe of the electronic nose was used to extract the gas from the headspace of the bottle for detection. Test parameters were set: sample flow rate of 300 mL/min, purge time of 120 s, and detection time of 120 s. It was observed that the sensors reached a steady state after 25 s of activation, hence a window from 29 to 31 s was selected for signal collection. Each sample was tested three times independently to ensure the reliability of the data.

2.8. Electronic tongue analysis

Referring to Zhou's method with slight modifications (Zhou et al., 2024), freeze-dried sample was configured to a concentration of 10 mg/mL, and 80 mL of it was taken for machine detection. Analysis conditions: automatic sampling, each sample was collected by sensors for 120 s, and each was tested 6 times. The data collected by the sensors at 120 s were used as the analysis data. The sensors of the electronic tongue (Alpha Mos, France) include AHS, CTS, NMS, PKS, CPS, ANS, SCS, a total of 7 sensors, among which AHS, ANS, CTS, NMS, and SCS sensors specifically recognize sour, sweet, salty, umami, and bitter tastes respectively.

2.9. Human sensory evaluation

The method was based on previous research and had been slightly modified. Twelve well-trained panel members (6 females and 6 males) with age between 20 and 30, were chosen from students of the Food Science College at Sichuan Agricultural University. They all voluntarily signed up to participate, and the monosodium glutamate used in this experiment were food grade, and the related experiments were approved by the Academic Ethical and Welfare Committee (Approval No. 20230308). They were all familiar with umami taste and owned experience in sensory evaluation. The participants involved in sensory evaluation received over 20 h of training. The panel members were tested with monosodium glutamate solutions at diverse concentrations (0.03, 0.09, 0.15, 0.21, 0.27, or 0.30 g/100 mL) for acclimating them to standard solution evaluation scale and umami taste intensity. 10 mg/mL sample solutions were maintained at 40 °C in water bath for avoiding temperature difference which possibly affected the evaluation. During the experiment, each tasting session began with rinsing the mouth with pure water, followed by a 10-min rest before continuing with the tasting. The panel members used an 11-point scale to assess the intensity of the umami taste. 1 indicates very weak, 6 indicates moderate, and 11 indicates very strong umami flavor (Phat et al., 2016).

2.10. Rheological analysis methods

With the approaches of Zeng et al. (Zeng et al., 2023), the rheological properties of Control, LEHs, and MRPs were studied using steady-state shear and dynamic frequency sweep methods (Discovery HR-1, TA

Co., USA). A parallel plate rheometer (40 mm diameter, steel) was used with a gap set at 1 mm and samples were equilibrated at 25 °C for 2 min before being measured. The shear viscosity experiments were done within the shear rate range of 0.1–100 s^{-1}. In the experiment, discoveries at the constant shear rate of 0.1–100 s^{-1} were reported, for straightly comparing apparent viscosities of diverse samples. Under conditions of an angular frequency of 10 s^{-1} and a temperature of 25 °C, linear viscoelastic region (LVR) of samples was defined through dynamic strain sweeps from 0.01 to 100 %. Then, within the linear viscoelastic range, frequency sweeps from 0.1 to 10 Hz were conducted at a fixed strain of 1 % at 25 °C. Discoveries are reported as storage modulus (G') and loss modulus (G″) as functions of frequency sweep.

2.11. Particle size & zeta potential measurement

The testing method was on basis of the approach of Zeng et al. (Zeng et al., 2023), with few changes, and each sample was tested three times. The lyophilized Control, LEHs, and MRPs were each prepared into a 1 mg/mL solution. Zeta potential and particle size of samples were measured via a dynamic light scattering nanometer particle size analyzer (Nano ZS, Malvern Panalytical, Malvern, UK), and PDI values were recorded.

2.12. Differential scanning calorimetry (DSC) detection methods

The method was slightly modified based on previous approach (X. Chen et al., 2021; Z. Chen et al., 2021). Thermal properties of lyophilized samples were determined through DSC (Q200MDSC, TA Co., USA). Around 8 mg of every sample was heated from 30 °C to 220 °C at 15 °C/min as the rate. One empty pan was used as the control. Thermal analysis data were analyzed and fitted using Advantage and Origin 2021 software, and the heat enthalpy calculations were based on the Speil equation.

2.13. Statistical analysis of data

The experimental results were statistically processed using SPSS 26 software, and the differences between groups were examined through Duncan's test ($P < 0.05$). Discoveries are presented as mean ± standard deviation. Graphing was done using Origin 2021. The electronic nose PCA and LDA diagrams were created using Winmuster.

3. Results and discussion

3.1. Free amino acids analysis

During the enzymatic hydrolysis process, some proteins are broken down into small peptides and amino acids, which impart flavor to the product and serve as precursors for the MR, affecting the color and flavor of final product (De Sousa Fontes et al., 2024; Zhao et al., 2018). In Table 1, altogether 25 amino acids were found. Among them, Control group contained the highest sum total of umami amino acids (Asp, Glu), at 22.3 mg/g. After enzymatic hydrolysis, aspartic acid content rose, but glutamic acid content decreased.

After the MR, the content of umami amino acids further decreased to 12.70 mg/g. It was also observed that following enzymatic hydrolysis, the total amount of free amino acids increased, with the content of bitte amino acids (Arg, His, Ile, Met, Leu, Phe, Val) rising from 61.82 mg/g to 102.81 mg/g, and the content of sweet amino acids (Ala, Gly, Ser, Thr) increasing from 32.81 mg/g to 36.28 mg/g. This increase is attributed to the cellulase initially disrupting some of the cell wall structure of the *Lentinula edodes*, allowing the subsequent action of the composite protease to be more effective on the proteins of the *Lentinula edodes*, thereby enhancing the release of amino acids (Zhao et al., 2019). However, after the MR, the total amount of free amino acids exhibited a decreasing trend, dropping from 242.94 mg/g to 133.94 mg/g, with the content of bitte amino acids and sweet amino acids respectively decreasing to 52.05 mg/g and 22.42 mg/g. The reduction in free amino acid content after the MR is primarily due to the reaction between amino acids and sugars, known as the Strecker degradation (Habinshuti et al., 2021; Zhang et al., 2022).

Table 1
Free amino acid content of Control, LEHs, and MRPs.

Amino acids	Samples/Content (mg/g)		
	Control	LEHs	MRPs
Asp	2.01 ± 0.16a	2.56 ± 0.21b	2.84 ± 0.04b
Glu	20.29 ± 1.06c	15.16 ± 0.94b	9.86 ± 0.24a
Asn	4.09 ± 0.14a	5.07 ± 0.43b	3.62 ± 0.08a
Ser	8.04 ± 0.06b	7.88 ± 0.61b	5.28 ± 0.09a
Gln	37.98 ± 0.20b	41.55 ± 3.37b	1.54 ± 0.05a
His	2.77 ± 0.19a	3.96 ± 0.05b	4.64 ± 0.11c
Gly	6.61 ± 0.40c	4.42 ± 0.29b	2.79 ± 0.04a
Thr	7.52 ± 0.28a	12.66 ± 0.88b	7.16 ± 0.10a
Cit	3.24 ± 0.27a	4.31 ± 0.17b	4.36 ± 0.02b
Arg	20.13 ± 0.25b	29.14 ± 1.88c	12.89 ± 0.23a
Ala	10.65 ± 0.29b	11.33 ± 0.76b	7.19 ± 0.11a
Tyr	2.46 ± 0.48b	2.22 ± 0.43b	0.28 ± 0.01a
Cys	0.55 ± 0.06a	1.14 ± 0.94a	5.57 ± 0.04b
Val	7.57 ± 0.43a	14.74 ± 1.45b	8.98 ± 0.21a
Met	11.28 ± 0.4b	13.5 ± 0.96c	3.66 ± 0.22a
Nva	0.88 ± 0.04b	1.32 ± 0.21c	0.56 ± 0.13a
Trp	1.15 ± 0.01a	1.70 ± 0.10b	2.28 ± 0.08c
Phe	4.94 ± 0.03a	11.39 ± 0.90c	7.70 ± 0.12b
Ile	3.66 ± 0.08a	10.00 ± 0.61c	6.20 ± 0.07b
Lys	10.14 ± 0.06a	21.24 ± 1.36b	11.50 ± 0.18a
Leu	11.48 ± 0.67b	20.08 ± 1.41c	7.98 ± 0.15a
Hyp	0.11 ± 0.02a	2.10 ± 0.43b	12.75 ± 0.27c
Sar	1.01 ± 0.48a	0.47 ± 0.07a	2.32 ± 0.03b
Pro	6.89 ± 0.19b	1.51 ± 0.65a	1.18 ± 0.06a
Gaba	2.80 ± 0.27b	3.49 ± 0.17c	1.84 ± 0.03a
Total free amino acids	188.21	242.94	133.94
MSG-like	22.30	17.72	12.70
Bitter	61.82	102.81	52.05
Sweet	32.81	36.28	22.42
Hydrophobic amino acids	57.62	84.26	45.17
Aromatic amino acids	8.55	15.24	10.28

Note: MSG-like = Asp + Glu; Bitter = Arg + His + Ile + Leu + Met + Phe + Val; Sweet = Ala + Gly + Ser + Thr; Hydrophobic amino acids = Phe + Leu + Ile + Met + Val + Trp + Pro ; Aromatic amino acids = Trp + Tyr + Phe; The numerical values are presented as the mean ± standard deviation of three repeated analyses. Significant differences among the values denoted by different lowercase superscript letters a-c within the same row are observed (Duncan, $P < 0.05$).

Arg, hydrophobic amino acids (Trp, Phe, Val, Leu, Ile, Ala, Pro, Met), and aromatic amino acids are closely related to antioxidant and hypoglycemic activities (Xu et al., 2023). Arginine and hydrophobic amino acids can bind to the active sites of α-amylase and α-glucosidase, forming van der Waals forces and hydrogen bonds, among other interactive forces, thereby inhibiting the activity of both enzymes, reducing glucose production, and consequently lowering blood glucose levels (Mirzapour-Kouhdasht et al., 2022; Xu et al., 2023). In the LEHs group, Arg, hydrophobic amino acids, and aromatic amino acids were the highest, with respective contents of 29.14 mg/g, 84.26 mg/g, and 15.24 mg/g, and all decreased after the MR. Aromatic amino acids (Trp, Tyr, Phe), which contain a benzene ring, are also associated with the antioxidant properties of the sample. In the structure of Tyr, there is a phenolic hydroxyl group, which can stabilize various forms of reactive oxygen species through electron resonance or delocalization effects, converting them into stable phenoxy radicals. This action can effectively inhibit free radical-induced peroxidation chain reactions, thereby protecting organisms from oxidative stress damage. In summary, the composition of amino acids is inseparable from the taste characteristics and biological activities of the sample solution (Dávalos et al., 2004; Tsopmo et al., 2011).

3.2. Flavor nucleotide content and succinic acid content

5'-IMP, 5'-GMP and 5'-AMP are common flavor nucleotides in edible mushrooms (Sun et al., 2020; Tsai et al., 2009). 5'-CMP and 5'-UMP have an auxiliary function in umami taste enhancement in the presence of monosodium glutamate (Zhao et al., 2019). Therefore, these nucleotides are vital for umami taste enhancement. As shown in Table 2, in the Control group, the content of 5'-IMP was 0.18 ± 0.005 mg/g. MRPs contain higher levels of 5'-CMP and 5'-UMP, which were 2.11 ± 0.02 mg/g and 1.77 ± 0.005 mg/g, respectively. 5'-AMP exhibited a higher content in the MRPs group (0.58 ± 0.003 mg/g) compared to other groups ($P<0.05$). In contrast, 5'-GMP was detected in all groups, with the highest concentration observed in the MRPs group (0.78 ± 0.017 mg/g) ($P<0.05$). This suggests that MR may be associated with the elevated levels of 5'-GMP. MR promoted flavor nucleotide content increase, possibly because of degradation of nucleic acids in mushrooms and the breakdown of ATP, releasing more 5'-GMP and 5'-AMP. Additionally, research by Dermiki et al. showed that the amount of 5'-AMP increased after treatment at 121 °C, suggesting that high temperature and pressure might facilitate the dissolution of this nucleotide (Dermiki et al., 2013). ATP is a precursor of nucleotides such as ADP and ATP, and the breakdown sequence is ATP → ADP → AMP → IMP → HxR → Hx (Zhu et al., 2021). The Control group contained more ATP (0.27 ± 0.002 mg/g) and ADP (4.88 ± 0.10 mg/g) was predominantly found in the LEHs group. The chemical structures of ATP and ADP are unstable, and during the reaction process, they easily convert to other related compounds, while HxR and Hx, as the final degradation products, were distributed in the Control, LEHs, and MRPs groups, indicating the degradation of 5'-AMP and 5'-IMP. In mushrooms, succinic acid is a major umami substance and can interact with other flavor components to enhance umami (Zhao et al., 2019). From Table 2, the Control group owned a succinic acid content of 76.86 ± 0.47 mg/kg, and the LEHs group had 86.02 ± 0.59 mg/kg, indicating that enzymatic hydrolysis effectively released succinic acid. The MRPs group had 87.35 ± 0.37 mg/kg, showing that the MR further released succinic acid, which corresponds with our previous LC-MS/MS data (Qiu et al., 2024).

3.3. Analysis of EUC value and TAV

EUC values can assist in understanding synergistic umami-enhancing effects between umami 5′-nucleotides and amino acids (Sun et al., 2020). Researchers have divided EUC values into four levels: > 1000 g MSG/100 g, 100–1000 g MSG/100 g, 10–100 g MSG/100 g, < 10 g MSG/100 g (Yang et al., 2022). Clearly, the Control (243.86 ± 13.81 g MSG/100 g), LEHs (275.15 ± 17.85 g MSG/100 g), and MRPs (293.84 ± 11.05 g MSG/100 g) were in the second category (100–1000 g MSG/100 g) as shown in Table 2. Enzymatic hydrolysis helped to increase the EUC value, mainly because it further liberates Asp and 5'-GMP. Although Maillard reaction decreased umami amino acids amount, the release of 5'-GMP and 5'-AMP resulted in no significant difference in EUC values between MRPs and LEHs ($P < 0.05$).

TAV can be utilized for determining the contribution of taste compounds to the overall taste profile and has been extensively applied in food flavor analyses (Yang et al., 2022). TAV values represent taste intensity, reflecting the contribution of compounds to taste strength; compounds having a TAV over 1 are regarded active in food flavor (Chen & Zhang, 2007). Therefore, the higher the TAV value, the larger the contribution of the compound to the overall taste intensity. In the Control group, TAV values of 5'-GMP, Asp, and Glu were all greater than 1, with Glu (405.73) having the highest TAV value. In the LEHs and MRPs groups, TAV values of 5'-GMP, Asp, and Glu were also greater than 1, with Glu having the highest values of 303.16 and 197.13 (Table 3), respectively. The results indicated that Glu contributes the most to the umami taste in Control, LEHs, and MRPs.

Table 2
Taste nucleotides (mg/g), succinic acid (mg/kg) content, and EUC value (g MSG/100 g) in Control, LEHs and MRPs.

	Control	LEHs	MRPs
5'-CMP	0.73 ± 0.016a	1.10 ± 0.003b	2.11 ± 0.02c
5'-UMP	0.21 ± 0.06b	Nd	1.77 ± 0.005c
5'-IMP	0.18 ± 0.005b	Nd	Nd
5'-GMP	0.32 ± 0.005a	0.61 ± 0.017b	0.78 ± 0.017c
5'-AMP	Nd	Nd	0.58 ± 0.003b
HX	0.86 ± 0.006a	1.54 ± 0.014b	2.94 ± 0.02c
HXR	1.86 ± 0.017c	3.28 ± 0.009a	2.20 ± 0.03b
ATP	0.27 ± 0.002c	0.22 ± 0.03b	Nd
ADP	2.94 ± 0.03b	4.88 ± 0.10c	1.91 ± 0.10a
EUC	243.86 ± 13.81a	275.15 ± 17.85b	293.84 ± 11.05b
Succinic acid	76.86 ± 0.47a	86.02 ± 0.59b	87.35 ± 0.37c
Total umami nucleotides	0.5	0.61	1.36

Note: Nd: not detected; Total umami nucleotides = 5'-IMP +5'-GMP + 5'-AMP; Significant differences among the values denoted by different lowercase superscript letters a-c within the same row are observed (Duncan, $P < 0.05$).

3.4. Sensory analysis

3.4.1. Analysis of electronic nose results

Fig. 1A shows the results after e-nose LDA analysis of different samples where LD1 and LD2 explained 75.822 % and 22.286 % of the variance in the data respectively, giving a cumulative explanation of 98.108 %. Similarly, the PCA also revealed that PC1 and PC2 occupy 74.648 % and 23.341 % of the variation, totaling 98.025 % (Fig. 1B). Both methods were effective in revealing the differences between samples. In terms of the distance between samples of the same species, all three samples showed high dispersion, indicating that different treatments had a large impact on volatile components of *Lentinula edodes*, which is consistent with our previous GC–MS results (Qiu et al., 2024).

The radar chart of flavor substance responses for different treatment groups is shown in Fig. 1C. The electronic nose has ten different metal oxide sensors (W1C: aromatic components, phenolics; W5S: nitrogen oxides; W3C: ammonia, aromatic compounds; W6S: selective to hydrides; W5C: short-chain alkanes, aromatic compounds; W1S: sensitive to methyl groups; W1W: inorganic sulfides; W2S: ethanol, aromatic compounds; W2W: aromatic, organic sulfides; W3S: long-chain alkanes). The results indicated that there existed differences in response values among the three samples across the ten sensors, and the response values also varied on the same sensor. Overall, the three samples showed the highest response values to the W2S sensor of the electronic nose, suggesting that the samples mostly consist of aromatic compounds, with the Control group having a tremendously greater content than the other two groups. The study found that Control group has the highest relative response value to W1S sensor, indicating that the Control group contains the most methyl-sensitive substances. The MRPs group showed higher response values to the W6S and W5S sensors, indicating that nitrogen

Table 3
Taste active value (TAV) of Control, LEHs and MRPs.

	Threshold (mg/g)	TAV		
		Control	LEHs	MRPs
5'-AMP	0.50	0	0	0.86 ± 0.06b
5'-IMP	0.25	0.73 ± 0.02b	0	0
5'-GMP	0.125	2.53 ± 0.04a	4.87 ± 0.13b	6.23 ± 0.14c
Asp	0.30	6.68 ± 0.54a	8.53 ± 0.69b	9.46 ± 0.14b
Glu	0.05	405.73 ± 21.21c	303.16 ± 18.84b	197.13 ± 4.78a
Succinic acid	0.11	0.70 ± 0.004a	0.78 ± 0.005b	0.79 ± 0.003c

Note: Threshold data were referenced from Wang's study (Wang et al., 2023). Significant differences among the values denoted by different lowercase superscript letters a-c within the same row are observed (Duncan, $P < 0.05$).

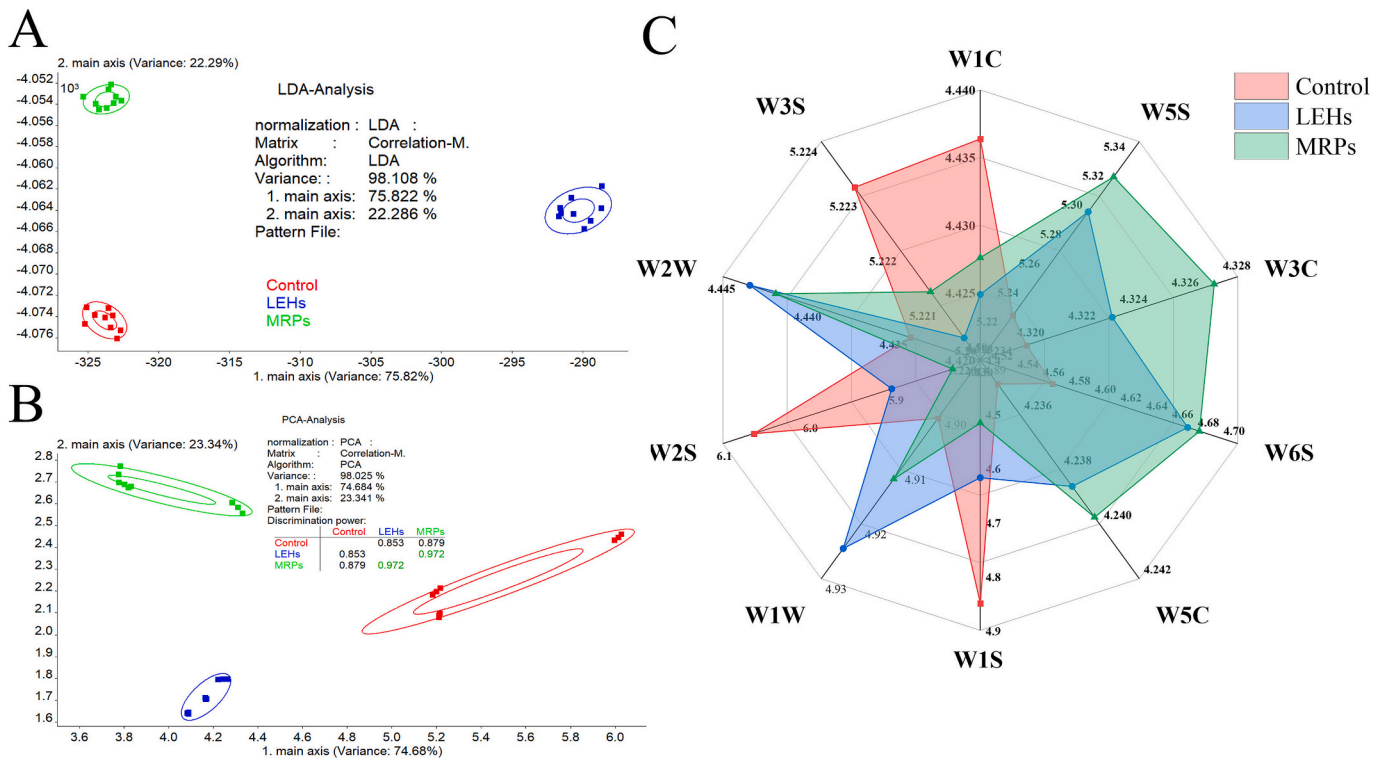

Fig. 1. Electronic nose analysis results for Control, LEHs and MRPs. (A): PCA. (B): LDA. (C): Radar plot of different sensor responses of the electronic nose.

oxides and hydrides were more present in the MRPs group. Additionally, MRPs had the highest relative response values to the W1W and W2W sensors compared to other groups, indicating that MRPs' volatile components contain more sulfur compounds, with cysteine being the most important sulfur source for these substances. In this MR system, pathways for the formation of sulfur-containing volatile compounds included the formation of Amadori products, Strecker degradation of cysteine, and the formation of its furan skeleton (Wang et al., 2012). Our previous research also found that MRPs generate sulfur-containing compounds represented by 3-methylthiopropanal, which can generate a meaty flavor and modulate the umami receptors T1R1/T1R3, vital for enhancing umami (Qiu et al., 2024; Toda et al., 2018).

3.4.2. *Analysis of electronic tongue results*

In Fig. 2A, PC1 and PC2 together contributed 98.4 %, with significant separation between Control, LEHs, and MRPs, indicating that water extraction, enzymatic hydrolysis, and Maillard reaction treatments had significant differences in the flavor presentation of *Lentinula edodes*. Fig. 2B shows that the signal strength of different sensors varied among different samples. The order of signal strength for sensor AHS was: LEHs > Control > MRPs, suggesting that the acidic substances were effectively dissociated after enzymatic hydrolysis, and reduced after the Maillard

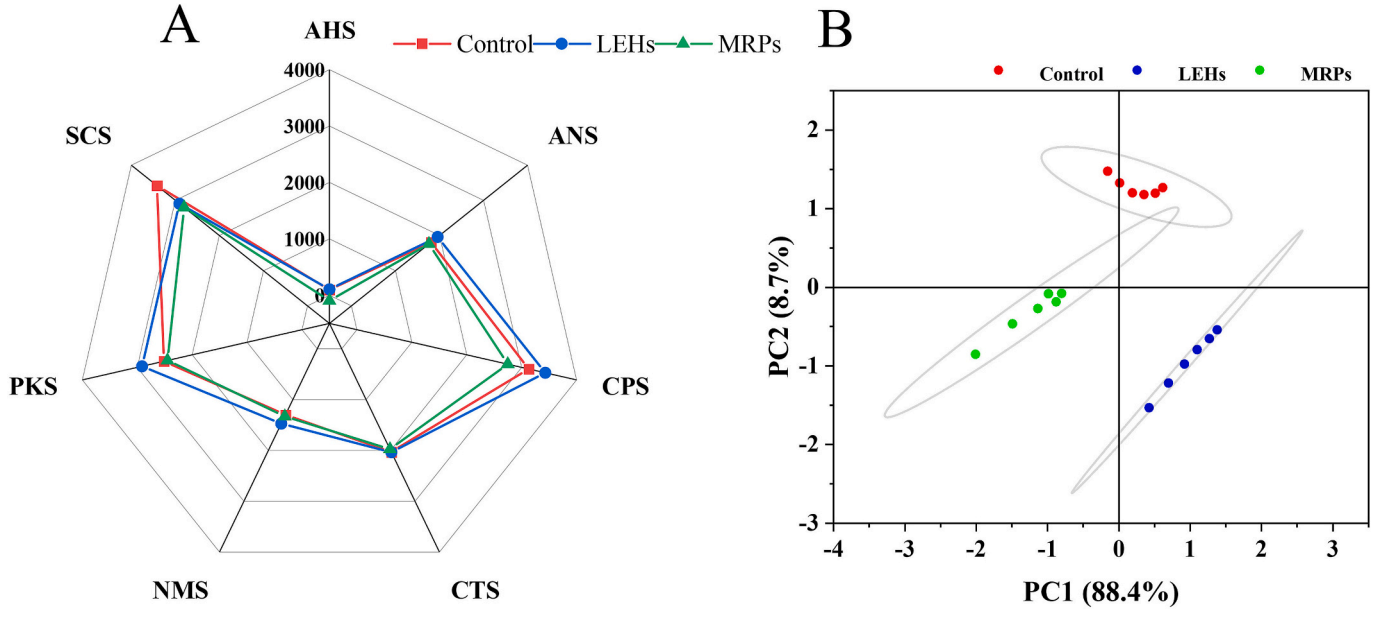

Fig. 2. Electronic tongue taste radargram (A) and PCA analysis (B) for Control, LEHs, and MRPs.

reaction, especially the acidic amino acids. For sensor ANS, the order was LEHs > Control > MRPs; cellulase partially dissociates the polysaccharides of *Lentinula edodes* cell walls into monosaccharides, increasing the sweetness of LEHs. Additionally, sweet amino acids were effectively dissociated after proteolytic hydrolysis, also increasing the sweetness. Due to the carbonyl-amino reaction, the sweetness of LEHs decreased after the MR. The signal intensity for sensor CTS showed no significant difference. The signal strength of sensor NMS indicated that LEHs had the strongest umami taste, suggesting that enzymatic hydrolysis freed umami amino acids, enhancing the umami flavor. The order of signal strength for sensor SCS was Control > LEHs > MRPs, indicating that the MR reduced bitterness, possibly because it decomposed bitter amino acids and other substances (Lan et al., 2010).

3.4.3. Human sensory evaluation

The results for sensory scoring and electronic tongue umami intensity are shown in Table 4. Sensory scoring indicates that MRPs had the highest score (6.25 ± 1.06) ($P < 0.05$); however, the electronic tongue showed a higher umami intensity for LEHs (1532.76 ± 48.09) ($P < 0.05$), indicating a discrepancy between the two. This discrepancy was due to the subjective nature of the sensory panelists (Dang et al., 2019). And it was mainly because the sensors of the electronic tongue might not recognize some umami peptides produced after enzymatic hydrolysis and the MR, leading to biased results. Additionally, research has revealed gases are also vital for modulating umami receptors (T1R1/T1R3), for example, 3-methylthiopropanal can conformationally modulate T1R1/T1R3 to enhance umami (Toda et al., 2018). The electronic tongue cannot simultaneously evaluate taste and smell, which was also a reason for the error in electronic sensory evaluation.

3.5. Rheological analysis

As shown in Fig. 3A, the viscosity of the samples decreased gradually with the increase in shear rate, exhibiting representative shear-thinning behavior. This mechanism can be attributed to the rupture or deformation of droplets and their clusters under shear force, leading to a decrease in viscosity (Zeng et al., 2023). The viscosity of LEHs was tremendously larger relative to the control, due to the degradation of polysaccharides from the cell wall of *Lentinula edodes* into monosaccharides during the enzymatic process. Additionally, the release of amino acids and peptides in *Lentinula edodes* also contributed to the increased viscosity of LEHs. After the MR, the viscosity of MRPs was tremendously larger relative to LEHs, due to addition of exogenous xylose during Maillard reaction process and the cross-linking of carbonyl compounds and amino compounds, which increased the viscosity of MRPs. Additionally, at high temperatures, some sugars dehydrate to produce caramel-like substances, which was also a reason for the increased viscosity of MRPs.

As frequency increases, storage modulus (G') and loss modulus (G") of the three samples showed an upward trend. G' reflects the elasticity of the sample, and G" reflects the viscosity of the sample (Du et al., 2012). In Control and LEHs, G" was always greater than G' (Fig. 3B), according to the formula for the loss angle tangent, tanδ = G"/G', where tanδ >1, indicating that the sample always exhibited viscous liquid behavior, suggesting that less content was dissolved in Control, and LEHs, due to enzymatic action, caused protein and polysaccharide degradation, leading to a decrease in gel properties. In MRPs, within the frequency scanning range of 0–7.5 Hz, the sample exhibits viscous behavior. Afterwards, G' was always greater than G", tanδ <1, the sample exhibited solid elastic properties, was gel-like, mainly due to glycosylation of proteins/peptides and sugars in the sample, improving the gel properties of the sample (Ke & Li, 2023; Kurt et al., 2016).

Table 4
Umami intensity of Control, LEHs, and MRPs based on electronic tongue and sensory evaluation.

Samples	Umami intensity	
	Electronic tongue test	Sensory evaluation
Control	1390.49 ± 65.22b	4.00 ± 0.85a
LEHs	1532.76 ± 48.09c	5.33 ± 1.07b
MRPs	1221.09 ± 101.15a	6.25 ± 1.06c

Note: Significant differences among the values denoted by different lowercase superscript letters a-c within the same row are observed (Duncan, $P < 0.05$).

3.6. Particle size & zeta potential analysis

PDI less than 0.30 usually indicates that the system consists of well-uniform particles (Shen et al., 2020). As shown in Fig. 4A, the PDIs of the Control, LEHs, and MRPs were all greater than 0.3, suggesting that these products still exhibited poor uniformity. The average particle size was 265.53 ± 11.70 nm for the Control group, 509.1 ± 10.36 nm for the LEHs, and 543.17 ± 17.75 nm for the MRPs. Particle size can reflect the size of particles in the solution and the aggregation of contents. The smallest particle size in the Control group may be due to the presence of *Lentinula edodes* cell walls, resulting in fewer extractable contents. After enzymatic hydrolysis, the contents within the cell walls were solubilized, leading to an increase in particle size for the LEHs. The addition of exogenous sugars and amino acids, along with the Maillard reaction, further increases the particle size due to the crosslinking reaction between reducing sugars and amino acids (Liu et al., 2024). Stability of colloids is tightly associated with their zeta potential, which reflects the repulsion among like-charged particles. As illustrated in Fig. 4B, the absolute value of the zeta potential for the MRPs solution (−13.6 ± 0.35 mV) was greater than that for the LEHs solution (−10.47 ± 0.25 mV), and tremendously larger relative to the Control group (−7.34 ± 0.78 mV) ($P < 0.05$), indicating that the solution post-Maillard reaction carried more negative charges. The reason for this phenomenon may be related to the negative charge of melanoidin (Qiu et al., 2024; RufiÁn-Henares & Cueva, 2009).

3.7. DSC analysis

The DSC analysis provides a reference for the temperature selection of hot air drying or spray drying in the processing of mushroom umami seasoning in the future. As shown in Table S1 (Supplementary Material 1), the temperatures at which the first thermochemical reactions occur for the Control, LEHs, and MRPs are 175.61 °C, 125.34 °C, and 125.99 °C, respectively. It was evident that the initial thermal denaturation temperatures of both LEHs and MRPs were lower relative to the Control. This might be associated with the fact that the main substances in the Control are proteins and polysaccharides, which were large molecular substances. Additionally, enzymatic hydrolysis process and MR disrupted spatial conformation and molecular structure of proteins, leading to a reduction in thermal denaturation temperature. The LEHs exhibited the fewest thermal peaks, which might be associated with the degradation of polysaccharides and proteins. Furthermore, the MRPs, being a mixture of complex components, displayed multiple thermal peaks, and these complex compounds underwent phase transitions as the temperature increased (Chen et al., 2021).

4. Conclusion

After the MR, umami amino acids content further diminished, but contents of umami nucleotides and succinic acid in the MRPs were relatively high. Enzymatic hydrolysis helped to increase the EUC value, while there was no significant difference after the MR. TAV indicated that 5'-GMP, Asp, and Glu were the key umami compounds in Control, LEHs, and MRPs, with Glu contributing the most to the umami taste of Control, LEHs, and MRPs. The sensory evaluation reflected that the MRPs have a strong umami taste. We also researched the influence of the MR on physicochemical properties of mushroom hydrolysates.

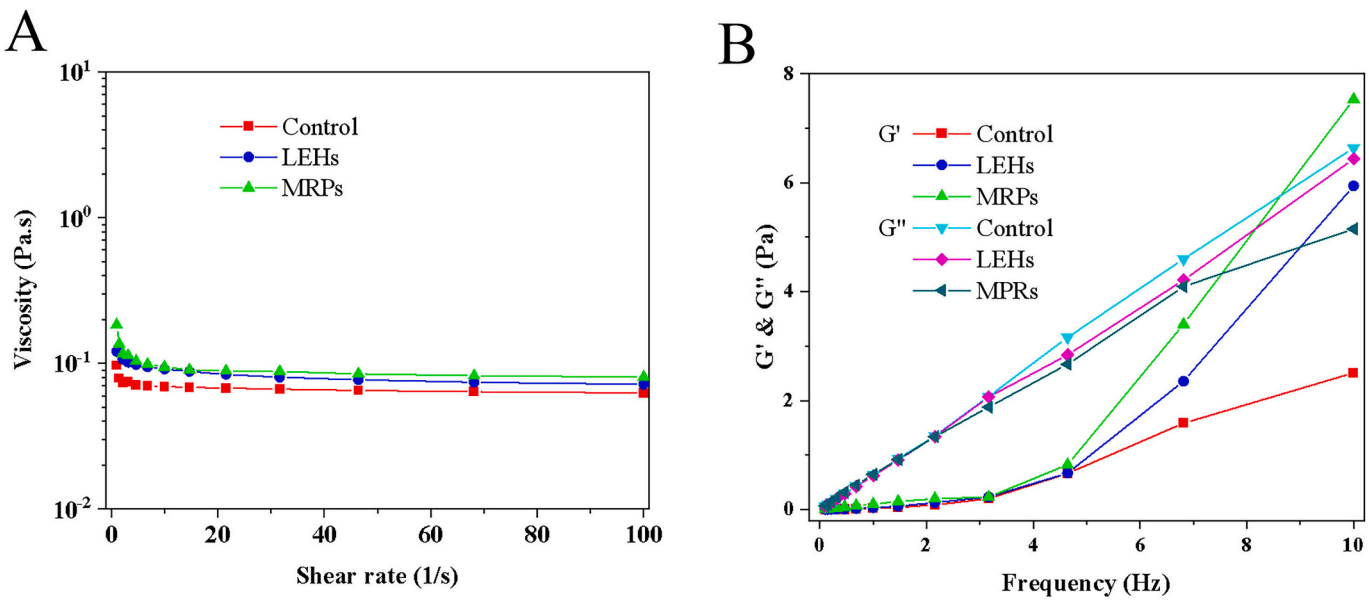

Fig. 3. Rheological properties of Control, LEHs, and MRPs. (A): Viscosity versus shear rate. (B): Variation curves of G' (energy storage modulus) and G" (loss modulus) with frequency.

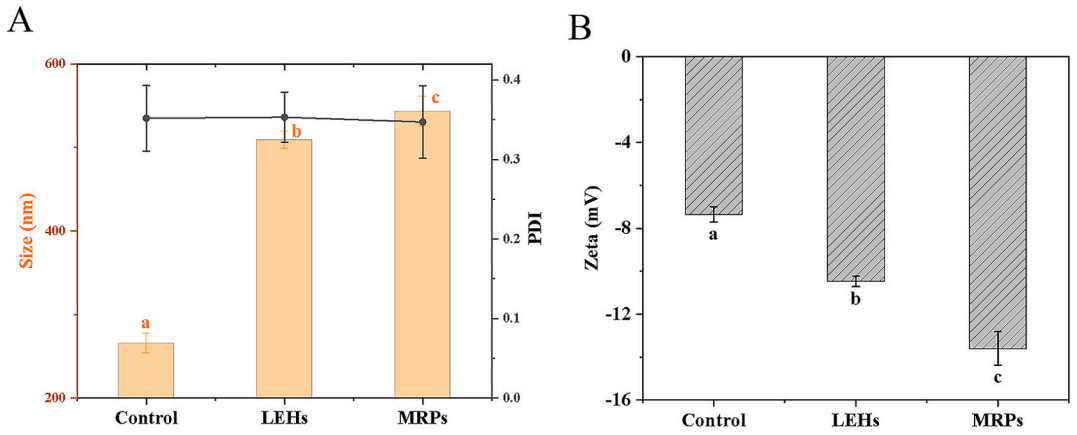

Fig. 4. Plot of particle size (A) and Zeta potential (B) for Control, LEHs, MRPs.

Discoveries displayed MR increased the particle size, absolute value of zeta potential, and viscosity of mushroom enzymatic hydrolysates. The critical temperatures for thermal chemical reactions were 125.34 °C and 125.99 °C for mushroom enzymatic hydrolysates and MRPs, respectively. In conclusion, these results laid a solid foundation for the application of the MR in the mushroom seasoning industry.

Ethical statement

This statement is to certify that all procedures performed in the study were in accordance with Sichuan Agricultural University Academic Ethical and Welfare Committee and with the 1964 Helsinki Declaration and its later amendments or comparable ethical standards (Approval No.20240308).

Statement of volunteer consent

The sensory experiments conducted in this study fully respected the wishes of the participants without any coercion, and all participants participated voluntarily. The experimental data obtained were disclosed to the participants, and no data of the participants were published without their knowledge. Volunteers read the informed consent form carefully, and the researchers explained the purpose, content, risks and benefits of the study to the volunteers in detail. Questions asked by the volunteers were answered. Volunteers were informed about the study and signed an informed consent form, and all volunteers agreed to participate in the study.

CRediT authorship contribution statement

Jianguo Qiu: Writing – original draft, Visualization, Methodology, Formal analysis. **Hongyu Li:** Visualization, Investigation. **Lijia Zhang:** Investigation. **Junqi Li:** Investigation. **Zhengfeng Fang:** Project administration, Funding acquisition. **Cheng Li:** Project administration, Funding acquisition. **Hong Chen:** Formal analysis. **Fahad Al-Asmari:** Resources. **Manal Y. Sameeh:** Resources. **Wenjuan Wu:** Supervision. **Yuntao Liu:** Supervision, Project administration, Funding acquisition, Conceptualization. **Zhen Zeng:** Validation, Supervision.

Declaration of competing interest

The authors declare that they have no known competing financial

interests or personal relationships that could influence the work reported in this paper.

Acknowledgments

The authors express their gratitude to the Key Project of the Chengdu Research and Development Project (2024-YF05-01937-SN), the Deanship of Scientific Research (DSR) at King Faisal University (project no. KFU241192), and the Key Project of the Chengdu-Chongqing Region Economic Circle of Agricultural Science and Technology Innovation Alliance.

Appendix A. Supplementary data

Supplementary data to this article can be found online at https://doi.org/10.1016/j.fochx.2024.101943.

Data availability

Data will be made available on request.

References

Altay, K., Sahingil, D., & Hayaloglu, A. A. (2024). A geographically-registered Arapgir purple basil pesto sauce prepared with four different cheese varieties: Comparison of physical, bioactive and rheological properties. *Food Chemistry Advances, 4*, Article 100587. https://doi.org/10.1016/j.focha.2023.100587

Andres-Hernando, A., Cicerchi, C., Kuwabara, M., Orlicky, D. J., Sanchez-Lozada, L. G., Nakagawa, T., … Lanaspa, M. A. (2021). Umami-induced obesity and metabolic syndrome is mediated by nucleotide degradation and uric acid generation. *Nature Metabolism, 3*, 1189–1201. https://doi.org/10.1038/s42255-021-00454-z

Chen, D.-W., & Zhang, M. (2007). Non-volatile taste active compounds in the meat of Chinese mitten crab (*Eriocheir sinensis*). *Food Chemistry, 104*, 1200–1205. https://doi.org/10.1016/j.foodchem.2007.01.042

Chen, X., Jiang, D., Xu, P., Geng, Z., Xiong, G., Zou, Y., Wang, D., & Xu, W. (2021). Structural and antimicrobial properties of Maillard reaction products in chicken liver protein hydrolysate after sonication. *Food Chemistry, 343*, Article 128417. https://doi.org/10.1016/j.foodchem.2020.128417

Chen, X., Yu, J., Cui, H., Xia, S., Zhang, X., & Yang, B. (2018). Effect of temperature on flavor compounds and sensory characteristics of Maillard reaction products derived from mushroom hydrolysate. *Molecules, 23*, 247. https://doi.org/10.3390/molecules23020247

Chen, Z., Gao, H., Wu, W., Chen, H., Fang, X., Han, Y., & Mu, H. (2021). Effects of fermentation with different microbial species on the umami taste of shiitake mushroom (*Lentinus edodes*). *LWT, 141*, Article 110889. https://doi.org/10.1016/j.lwt.2021.110889

Dang, Y., Hao, L., Zhou, T., Cao, J., Sun, Y., & Pan, D. (2019). Establishment of new assessment method for the synergistic effect between umami peptides and monosodium glutamate using electronic tongue. *Food Research International, 121*, 20–27. https://doi.org/10.1016/j.foodres.2019.03.001

Dávalos, A., Miguel, M., Bartolomé, B., & López-Fandiño, R. (2004). Antioxidant activity of peptides derived from egg white proteins by enzymatic hydrolysis. *Journal of Food Protection, 67*, 1939–1944. https://doi.org/10.4315/0362-028x-67.9.1939

De Sousa Fontes, V. M., De Sousa Galvão, M., Moreira De Carvalho, L., Guedes, D. N., & F. L., Dos Santos Lima, M., Alencar Bezerra, T. K., & Madruga, M. S.. (2024). Thiamine, cysteine and xylose added to the Maillard reaction of goat protein hydrolysate potentiates the formation of meat flavoring compounds. *Food Chemistry, 445*, Article 138398. https://doi.org/10.1016/j.foodchem.2024.138398

Dermiki, M., Phanphensophon, N., Mottram, D. S., & Methven, L. (2013). Contributions of non-volatile and volatile compounds to the umami taste and overall flavour of shiitake mushroom extracts and their application as flavour enhancers in cooked minced meat. *Food Chemistry, 141*, 77–83. https://doi.org/10.1016/j.foodchem.2013.03.018

Du, X., Li, J., Chen, J., & Li, B. (2012). Effect of degree of deacetylation on physicochemical and gelation properties of konjac glucomannan. *Food Research International, 46*, 270–278. https://doi.org/10.1016/j.foodres.2011.12.015

Habinshuti, I., Mu, T.-H., & Zhang, M. (2021). Structural, antioxidant, aroma, and sensory characteristics of Maillard reaction products from sweet potato protein hydrolysates as influenced by different ultrasound-assisted enzymatic treatments. *Food Chemistry, 361*, Article 130090. https://doi.org/10.1016/j.foodchem.2021.130090

Ke, C., & Li, L. (2023). Influence mechanism of polysaccharides induced Maillard reaction on plant proteins structure and functional properties: A review. *Carbohydrate Polymers, 302*, Article 120430. https://doi.org/10.1016/j.carbpol.2022.120430

Kong, Y., Wu, Z., Li, Y., Kang, Z., Wang, L., Xie, F., & Yu, D. (2024). Analyzing changes in volatile flavor compounds of soy protein isolate during ultrasonic-thermal synergistic treatments using electronic nose and HS-SPME-GC-MS combined with chemometrics. *Food Chemistry, 445*, Article 138795. https://doi.org/10.1016/j.foodchem.2024.138795

Kurt, A., Cengiz, A., & Kahyaoglu, T. (2016). The effect of gum tragacanth on the rheological properties of salep based ice cream mix. *Carbohydrate Polymers, 143*, 116–123. https://doi.org/10.1016/j.carbpol.2016.02.018

Lan, X., Liu, P., Xia, S., Jia, C., Mukunzi, D., Zhang, X., Xia, W., Tian, H., & Xiao, Z. (2010). Temperature effect on the non-volatile compounds of Maillard reaction products derived from xylose–soybean peptide system: Further insights into thermal degradation and cross-linking. *Food Chemistry, 120*, 967–972. https://doi.org/10.1016/j.foodchem.2009.11.033

Liu, Y., Guo, X., Liu, T., Fan, X., Yu, X., & Zhang, J. (2024). Study on the structural characteristics and emulsifying properties of chickpea protein isolate-citrus pectin conjugates prepared by Maillard reaction. *International Journal of Biological Macromolecules, 264*, Article 130606. https://doi.org/10.1016/j.ijbiomac.2024.130606

Manninena, H., Rotola-Pukkilab, M., Aisalac, H., Hopiab, A., & Laaksonena, T. (2018). Free amino acids and 5′-nucleotides in Finnish forest mushrooms. *Food Chemistry, 247*, 23–28. https://doi.org/10.1016/j.foodchem.2017.12.014

Mirzapour-Kouhdasht, A., Garcia-Vaquero, M., Eun, J.-B., & Simal-Gandara, J. (2022). Influence of enzymatic hydrolysis and molecular weight fractionation on the antioxidant and lipase / α-amylase inhibitory activities in *vitro* of watermelon seed protein hydrolysates. *Molecules, 27*, 7897. https://doi.org/10.3390/molecules27227897

Phat, C., Moon, B., & Lee, C. (2016). Evaluation of umami taste in mushroom extracts by chemical analysis, sensory evaluation, and an electronic tongue system. *Food Chemistry, 192*, 1068–1077. https://doi.org/10.1016/j.foodchem.2015.07.113

Qiu, J., Li, H., Liu, Y., Li, C., Fang, Z., Hu, B., Li, X., Zeng, Z., & Liu, Y. (2024). Changes in flavor and biological activities of *Lentinula edodes* hydrolysates after Maillard reaction. *Food Chemistry, 431*, Article 137138. https://doi.org/10.1016/j.foodchem.2023.137138

RufiÁn-Henares, J. A., & Cueva, S. P. D. L. (2009). Antimicrobial activity of coffee melanoidins—A study of their metal-chelating properties. *Journal of Agricultural and Food Chemistry, 57*, 432–438. https://doi.org/10.1021/jf8027842

Shen, P., Zhou, F., Zhang, Y., Yuan, D., Zhao, Q., & Zhao, M. (2020). Formation and characterization of soy protein nanoparticles by controlled partial enzymatic hydrolysis. *Food Hydrocolloids, 105*. https://doi.org/10.1016/j.foodhyd.2020.105844

Sun, L.-B., Zhang, Z.-Y., Xin, G., Sun, B.-X., Bao, X.-J., Wei, Y.-Y., Zhao, X.-M., & Xu, H.-R. (2020). Advances in umami taste and aroma of edible mushrooms. *Trends in Food Science & Technology, 96*, 176–187. https://doi.org/10.1016/j.tifs.2019.12.018

Toda, Y., Nakagita, T., Hirokawa, T., Yamashita, Y., Nakajima, A., Narukawa, M., Ishimaru, Y., Uchida, R., & Misaka, T. (2018). Positive/negative allosteric modulation switching in an umami taste receptor (T1R1/T1R3) by a natural flavor compound, methional. *Scientific Reports, 8*, 11796. https://doi.org/10.1038/s41598-018-30315-x

Tsai, S.-Y., Huang, S.-J., Lo, S.-H., Wu, T.-P., Lian, P.-Y., & Mau, J.-L. (2009). Flavour components and antioxidant properties of several cultivated mushrooms. *Food Chemistry, 113*, 578–584. https://doi.org/10.1016/j.foodchem.2008.08.034

Tsopmo, A., Romanowski, A., Banda, L., Lavoie, J. C., Jenssen, H., & Friel, J. K. (2011). Novel anti-oxidative peptides from enzymatic digestion of human milk. *Food Chemistry, 126*, 1138–1143. https://doi.org/10.1016/j.foodchem.2010.11.146

Wang, J., Jiang, S., Miao, S., Zhang, L., Deng, K., & Zheng, B. (2023). Effects of drying on the quality characteristics and release of umami substances of *Flammulina velutipes*. *Food Bioscience, 51*, Article 102338. https://doi.org/10.1016/j.fbio.2022.102338

Wang, R., Yang, C., & Song, H. (2012). Key meat flavour compounds formation mechanism in a glutathione–xylose Maillard reaction. *Food Chemistry, 131*, 280–285. https://doi.org/10.1016/j.foodchem.2011.08.079

Xu, Y., Yang, Y., Ma, C.-M., Bian, X., Liu, X.-F., Wang, Y., Chen, F.-L., Wang, B., Zhang, G., & Zhang, N. (2023). Characterization of the structure, antioxidant activity and hypoglycemic activity of soy (*Glycine max L.*) protein hydrolysates. *Food Research International, 173*, Article 113473. https://doi.org/10.1016/j.foodres.2023.113473

Yang, F., Lv, S., Liu, Y., Bi, S., & Zhang, Y. (2022). Determination of umami compounds in edible fungi and evaluation of salty enhancement effect of antler fungus enzymatic hydrolysate. *Food Chemistry, 387*, Article 132890. https://doi.org/10.1016/j.foodchem.2022.132890

Zeng, Z., Deng, S., Liu, Y., Li, C., Fang, Z., Hu, B., Chen, H., Wang, C., Chen, S., Wu, W., & Liu, Y. (2023). Targeting transportation of curcumin by soybean lipophilic protein nano emulsion: Improving its bioaccessibility and regulating intestinal microorganisms in mice. *Food Hydrocolloids, 142*, Article 108781. https://doi.org/10.1016/j.foodhyd.2023.108781

Zhang, J., Sun-Waterhouse, D., Su, G., & Zhao, M. (2019). New insight into umami receptor, umami/umami-enhancing peptides and their derivatives: A review. *Trends in Food Science & Technology, 88*, 429–438. https://doi.org/10.1016/j.tifs.2019.04.008

Zhang, W., Han, Y., Shi, K., Wang, J., Yang, C., & Xu, X. (2022). Effect of different sulfur-containing compounds on the structure, sensory properties and antioxidant activities of Maillard reaction products obtained from *Pleurotus citrinopileatus* hydrolysates. *LWT, 171*, Article 114144. https://doi.org/10.1016/j.lwt.2022.114144

Zhao, T., Zhang, Q., Wang, S., Qiu, C., Liu, Y., Su, G., & Zhao, M. (2018). Effects of Maillard reaction on bioactivities promotion of anchovy protein hydrolysate: The key role of MRPs and newly formed peptides with basic and aromatic amino acids. *LWT, 97*, 245–253. https://doi.org/10.1016/j.lwt.2018.06.051

Zhao, Y., Zhang, M., Devahastind, S., & Liu, Y. (2019). Progresses on processing methods of umami substances: A review. *Trends in Food Science & Technology, 93*, 125–135. https://doi.org/10.1016/j.tifs.2019.09.012

Zheng, S., Ye, P., Zhao, X., Li, W., & Hou, L. J. F. R. I. (2023). Enhanced soy sauce stability and reduced precipitation by improving critical steps in the fermentation process. *Food Research International, 174*, Article 113674. https://doi.org/10.1016/j.foodres.2023.113674

Zhou, Y., Zhang, Z., He, Y., Gao, P., Zhang, H., & Ma, X. (2024). Integration of electronic nose, electronic tongue, and colorimeter in combination with chemometrics for monitoring the fermentation process of *Tremella fuciformis*. *Talanta, 274*, Article 126006. https://doi.org/10.1016/j.talanta.2024.126006

Zhu, W., Luan, H., Bu, Y., Li, J., Li, X., & Zhang, Y. (2021). Changes in taste substances during fermentation of fish sauce and the correlation with protease activity. *Food Research International, 144*, Article 110349. https://doi.org/10.1016/j.foodres.2021.110349